Creating and Stabilizing an Oxidized Pd Surface under Reductive Conditions for Photocatalytic Hydrogenation of Aromatic Carbonyls

Wei Qiao[1,2#], Xing Fan[3#], Weifeng Liu[4#], Fahir Niaz Khan[1], Dongsheng Zhang[1,2], Feiyu Han[1,2], Huiyu Yue[1], Yajiao Li[1], Nikolaos Dimitratos[4,5], Stefania Albonetti[4,5], Xiaodong Wen[2,6], Yong Yang[2,6], Flemming Besenbacher[7], Yongwang Li[2,6], Hans Niemantsverdriet[2,8], Haiping Lin[9,*], Ren Su[1,2,*]

[1] Soochow Institute for Energy and Materials Innovations (SIEMIS), Soochow University, Suzhou, 215006, China

[2] SynCat@Beijing, Synfuels China Technology Co. Ltd., Leyuan South Street II, No.1, Beijing, 101407, China

[3] Research Center for Carbon-based Electronics and Key Laboratory for the Physics and Chemistry of Nanodevices, School of Electronics, Peking University, Beijing 100871, China

[4] Dipartimento di Chimica Industriale "Toso Montanari", University of Bologna, Bologna 40136, Italy

[5] Center for Chemical Catalysis-C3, Alma Mater Studiorum University of Bologna, Bologna 40136, Italy

[6] State Key Laboratory of Coal Conversion, Institute of Coal Chemistry, CAS, Taiyuan, 030001, China

[7] The Interdisciplinary Nanoscience Center (iNANO), Aarhus University, DK-8000 Aarhus, Denmark

[8] SynCat@DIFFER, Syngaschem BV, 6336 HH Eindhoven, The Netherlands

[9] School of Physics and Information Technology, Shaanxi Normal University, Xi'an, 710119, China

Supporting Methods

1. Supporting Notes

Supporting Note 1. DFT calculations.

All theoretical calculations in this work were based on the periodic density functional theory (DFT) using Vienna Ab-initio Simulation Package (VASP) code [1,2].

The electron-ion interactions were treated within the projector augmented-wave (PAW) approximation[3,4]. The exchange-correlation functional was described by the Perdew, Burke, and Ernzerhof (PBE) parameterization of the generalized gradient approximation (GGA) [5,6]. A cutoff energy of 400 eV was employed for the plane-wave basis set of all calculations. The metallic Pd was mimicked with a (6 × 6 × 4) Pd(111) slab. The partially hydrogenated Pd was modelled with the aforementioned Pd(111) surface with 9 H atom adsorbed at the hollow sites. This structure is referred to as the $Pd_{36}H_9$ in this work. The PdO catalyst was modelled with a PdO(101) slab, consisting of 120 Pd and 120 O atoms. During structural optimizations, only the top two periodic layers were allowed to relax in three dimensions, and the bottom two layers were restricted. Ten relaxed ethanol molecules were added to fill the vacuum region close to the Pd-based surfaces to mimic the liquid ethanol solvent. The structure relaxation was reached until the residual force was below 0.01 eV $Å^{-1}$. The Brillouin zone was sampled by a 2 × 2 × 1 k-point sampling for the periodic Pd-based surface models and a 1 × 1 × 1 k-point sampling for isolated molecules. All periodic surface models were placed in cubic supercells with lattice parameter c = 30 Å in the z direction to avoid interactions between periodic images. An empirical correlation (DFT-D3) was employed to describe the van der Waals interactions[7]. The adsorption energies of molecules on the various Pd-based surfaces were calculated according to the following equation:

$$E_{ads} = E(\text{adsorbed system}) - E(\text{desorbed system}) \quad \text{Eq. S1}$$

The change of the Gibbs free energy (ΔG) for each elementary step at the zero potential were calculated using the following equation:

$$\Delta G = \Delta E + \Delta E_{ZPE} - T\Delta S \quad \text{Eq. S2}$$

where E was the total energy obtained directly from the DFT calculations. E_{ZPE} and S were the zero-point energy and the entropy, respectively. T was the temperature (298.15 K).

Supporting Note 2. Synthesis of Pd supported photocatalysts

Raw Materials: The following commercial precursors were applied: Melamine monomer and cyanuric acid (98.0%, TCI Shanghai Co. Ltd.); $PdCl_2$, $AgNO_2$, $HAuCl_4·3H_2O$, $CuCl_2$, $H_2PtCl_6·6H_2O$, $Cd(NO_3)_2·4H_2O$, NH_2CSNH_2 and ethylenediamine (analytic grade, Shanghai Aladdin Bio-Chem Technology Co. Ltd.); NaOH (97%, Saen Chemical Technology Co. Ltd.); $NaBH_4$ (analytic grade, Alfa Aesar (China) Chemical Co. Ltd.). All chemicals were used as received without further purification.

The graphitic carbon nitride (CN): The CN was synthesized by a thermal condensation method according to the literature[8]. Melamine monomer (1 g) and cyanuric acid (5 g) powders were loaded in a crucible with a lid and calcined in a muffle oven at 550 °C for 4 h using a ramping rate of 5 $°C·min^{-1}$ and then cooled to room temperature (RT) naturally.

Pd(II)/CN: A modified photo-deposition method was utilized to prepare the Pd(II)/CN using the setup shown in Supporting Scheme S1. Firstly, 0.4 g of CN and calculated amount of $PdCl_2$ (Pd loading: 3 wt%) were added in 15 mL of absolute ethanol (99.7 vol%), sonicated for 0.5 h to obtain a homogenous suspension. After sonication, 10 mL DI water was added into the 15 mL suspension, which was deaerated by N_2 purging for three times under magnetic stirring. A LED (410 nm, 150 mW) lamp was then employed to irradiate the suspension at RT for 5 h under

deaerated conditions. The P**d**(II)/**CN** suspension was centrifuged and washed with DI water and ethanol for 3 times, and finally the powders were dried in a vacuum oven at 60 °C for 12 h.

PdH_X/CN: A modified photo-deposition method was utilized to prepare the PdH_X/CN using the setup shown in Supporting Scheme S1. Firstly, 0.4 g of CN and calculated amount of $PdCl_2$ (Pd loading: 3 wt%) were added in 25 mL of absolute ethanol (99.7 vol%), sonicated for 0.5 h to obtain a homogenous suspension. The suspension was deaerated by Ar purging for three times under magnetic stirring. A LED (410 nm, 150 mW) lamp was then employed to irradiate the suspension at RT for 10 h under deaerated conditions. The PdH_X/CN suspension was centrifuged and washed with DI water and ethanol for 3 times, and finally the powders were dried in a vacuum oven at 60 °C for 12 h.

Pd/TiO_2: A modified photo-deposition method was utilized to prepare the Pd/TiO_2 using the setup shown in Supporting Scheme S1. Firstly, 1.0 g of TiO_2 and calculated amount of $PdCl_2$ (Pd loading: 1 wt%) were added in 15 mL isopropanol and 10 mL DI H_2O, which was then stirred for 0.5 h to obtain a homogenous suspension. After stirring, the slurry was deaerated by N_2 gas for three times under magnetic stirring. A LED (365 nm, 150 mW) lamp was then employed to irradiate the suspension at RT for 1.5 h under deaerated conditions. The Pd/TiO_2 suspension was centrifuged and washed with DI water and ethanol for 3 times, and finally the powders were dried in an oven at 50 °C for 3 h.

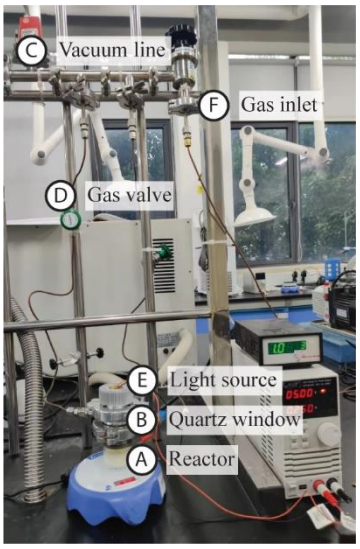

Supporting Scheme S1. Setup for photodeposition of Pd cocatalyst on semiconductor photocatalyst.

Supporting Note 3. Calculation of quantum efficiency (QE)

The setup for QE analysis can be found in our previous work and Supporting Scheme S1[9]. The QE of photocatalytic hydrogenation of benzaldehyde to toluene is calculated according to Eq. S3:

$$QE = \frac{n_{electrons}}{n_{photons}} = \frac{n_T * \text{Con.} * Sel. * N_A * i_e}{\Phi * t_R} * 100\% \quad \text{Eq. S3}$$

where $n_{electrons}$ and $n_{photons}$ are the total numbers of consumed electrons and incident photons; The n_T is the initial molar number of toluene ($81*10^{-6}$ mol); Con. and Sel. are the conversion of benzaldehyde (>99%) and selectivity to toluene (>99%) at the set irradiation time (t_R = 50 min); N_A is the Avogadro constant, i_e is the number of electrons for converting one part of benzaldehyde to toluene molecule (4). Φ is the photon flux of the light source of the 410 nm LED.

The number of incident photons is calculated according to Eq. S4:

$$n_{photons} = \frac{W_{lamp} * \lambda * t_R}{h * c} \quad \text{Eq.}$$

S4

where W_{lamp} and λ are the light intensity (300 mW) and wavelength (410 nm) of the LED lamp, *h* is the Planck constant (6.626 *10^{-34} J□s) and c is the speed of the light (3.0 *10^{8} m□s^{-1}).

The estimated $n_{photons}$ and $n_{electrons}$ are 1.875*10^{21} and 1.911*10^{20}, respectively. Therefore, the estimated QE is ~10.2%.

Supporting Note 4. *In-situ* MS analysis.

The evolution of gas phase products was monitored by a quadruple mass spectrometer (MS, HPR-20, Hiden) equipped with an *in-situ* reactor. In this reaction system, a reaction chamber with a quartz window was connected to the mass spectrometer *via* a leak-valve. The analysis was carried out using a reaction mixture that consists of 50 mg photocatalyst and 10 mM benzaldehyde in 10 mL ethanol. Control experiments in the absence of benzaldehyde were also performed for comparison. Before irradiation, the reactor was evacuated and then filled with Ar gas. A purple LED (410 nm, 350 mW) was utilized as the light source.

Detailed information is available in our previous publications[10]. The mass to charge ratios (m/e^-) of 44, 32, 28, 18 and 2 are measured to monitor the evolution of carbon dioxide, oxygen, nitrogen, water and hydrogen, respectively.

The hydrogen evolution was quantitative calculated using the following equations:

$$n(H_2) = \frac{p(H_2)_{reactor} * V_{reactor}}{R * T}$$ Eq. S5

$$p(H_2)_{reactor} = \frac{RSF(H_2) * p(H_2)_{detector} * p(Air)_{reactor}}{p(Air)_{detector}}$$ Eq. S6

where

$p(H_2)_{reactor}$ is the partial pressure of H_2 in the reactor;

$p(H_2)_{detector}$ is the measured partial pressure of H_2 determined by the mass spectrometer in the vacuum chamber;

$p(Air)_{reactor}$ is the pressure of ambient air (N_2 + O_2) in the reactor (101 kPa);

$p(Air)_{detector}$ is the measured pressure of air (N_2 + O_2) determined by the mass spectrometer in the vacuum chamber;

$V_{reactor}$ is the volume of the reactor excluding the liquid volume (~200 mL);

$RSF(H_2)$ is the relative sensitivity factor of H_2 (0.4 in ambient pressure);

2. Physical and chemical characterizations

2.1 X-ray Photoelectron Spectroscopy (XPS)

The surface chemical compositions of the samples and oxidation states of each element were investigated using an X-ray photoelectron spectrometer (PHI 5000 VersaProbe □, ULVAC-PHI) equipped with a monochromatic Al Kα X-ray source. Survey scans were measured using the following parameters: energy scan range of 1200 to -10 eV, pass energy of 160 eV, dwell time of 0.1 s, step size of 1 eV, and scan numbers of 3 times. For the region-of-interest spectra (C1s, N1s, Pd3d and O1s), a pass energy of 40 eV and a step size of 0.1 eV with a dwell time of 0.5 s were utilized. Adventitious C (C1s = 284.6 eV) was employed for calibration.

2.2 N_2 adsorption/desorption isotherm

The Brunauer-Emmett-Teller (BET) surface area of samples was obtained by the nitrogen adsorption/desorption isotherms measured at 77 K on a Micromeritics TriStar□3020 system.

2.3 Powder X-ray Diffraction (PXRD)

PXRD data were collected on a Bruker D8 Advance diffractometer equipped with a Cu anode (40 kV, 40 mA). The PXRD patterns were recorded in the scan range of 10-80°, a step size of 0.02° and a dwell time of 0.5 s. For the

fine diffraction pattern, a scan range of 37-41°, a step size of 0.01° and a dwell time of 5 s.

2.4 Transmission electron microscopy (TEM)

The microstructural information of the photocatalyst was studied using a transmission electron microscope (FEI Titan ThemisZ) operated at 120 kV. The sample was added into 1 mL of alcohol and sonicated for 5 min to form a suspension. A drop of the suspension was cast on the Cu stage and dried in air.

2.5 Electron paramagnetic resonance (EPR)

The radical species generated during the photocatalytic reduction of benzaldehyde were analyzed by EPR using an X-band JES-X320 spectrometer in the range of 321-331 mT at RT. A modulation width of 0.14 mT and an amplitude of 200 was used for all measurements. The 5,5-dimethyl-1-pyrroline N-oxide (DMPO) was utilized as the spin-trapping reagent.

2.6 Temperature programmed desorption-mass spectrometry (TPD-MS)

TPD-MS was utilized to analyze the adsorption of benzaldehyde and acetal on Pd(II)/CN and PdH_x/CN using a chemisorption analyzer (AutoChem II) coupled with a MS (OmniStar GSD, Pfeiffer). The process is as the following: Firstly, fresh photocatalyst powders (30 mg) were placed in a closed chamber and purged with Ar gas for 30 minutes to ensure a clean surface of the photocatalyst. Then the organic compounds (5 mL) were introduced to the photocatalyst chamber for 1 h *via* Ar purging. Next, the inlet valve was closed and the photocatalyst were kept in organic compound/Ar atmosphere for another 6 h. Finally, the photocatalyst powders were loaded into a U-shaped quartz tube in a chemisorption analyzer. To start the TPD test the loaded sample was heated to 500 °C at a ramp rate of 10 °C·min^{-1} with a He flow rate of 50 mL·min^{-1}. Meanwhile the desorbed gases were monitored by the coupled MS in real time.

2.7 Apparatus for photocatalyst screening and substrate scope

The photocatalytic conversion of aromatic carbonyls was performed in a multichannel reaction system with six Pyrex-glass-made reactors (SUNCAT INSTRUMENTS, China). The setup consists of three parts: A circular 410 nm LED light source with magnetic stir base, a DC power supply, and a cooling system for the light source. Each of the reactor contains 2 mL of alcohol with 10 mg photocatalyst and 10 mM reactant, which was purged and filled with Ar before irradiation. Details of the reaction system can be found in our previous work[11].

After reaction, the suspension was centrifuged and the aliquots were analyzed by gas chromatography (Agilent GC 8860) and combined gas chromatography and mass spectrometry (GC-MS, Agilent 8860 GC system coupled with a 5977B mass selective detector). An HP-5 MS column and an FID detector were equipped in the GC-MS.

2.8 Thermocatalytic conversion of benzaldehyde

The thermocatalytic conversion of benzaldehyde was performed in ethanol under deaerated conditions at 60 °C in an oil bath using Pd(II)/CN, Pd/TiO_2, and Pd/C catalyst. In specific, 10 mg catalyst powders were added into 2 mL of ethanol that contains 10 mM benzaldehyde, which was purged and filled with Ar at RT before reaction. After reaction at 60 °C for 50 min, the suspension was centrifuged and the aliquots were analyzed by GC-MS.

3. Supporting figures

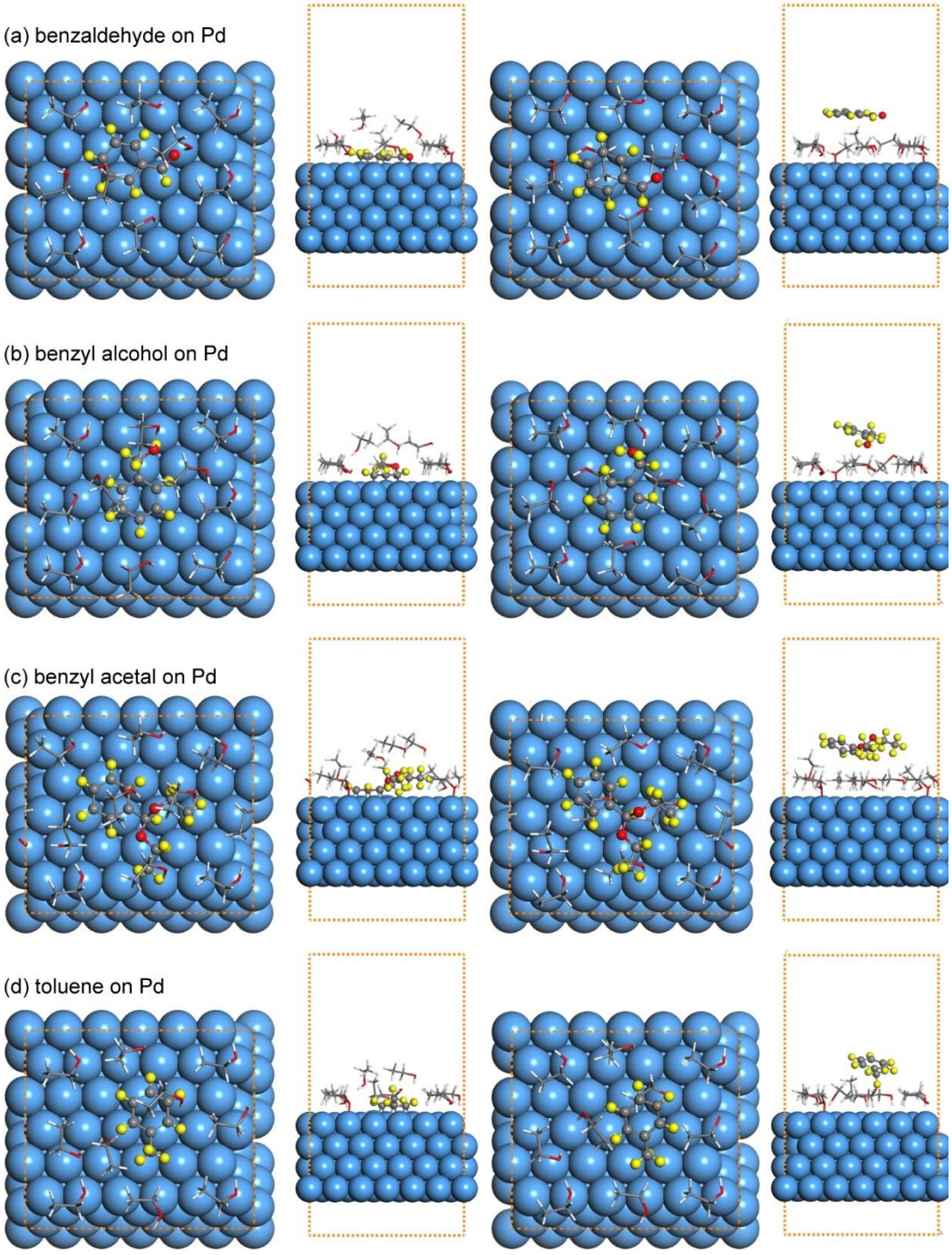

Supporting Figure S1. Optimized adsorption configurations of reactants, intermediates, and products with ten ethanol molecules on Pd surface by DFT calculations.

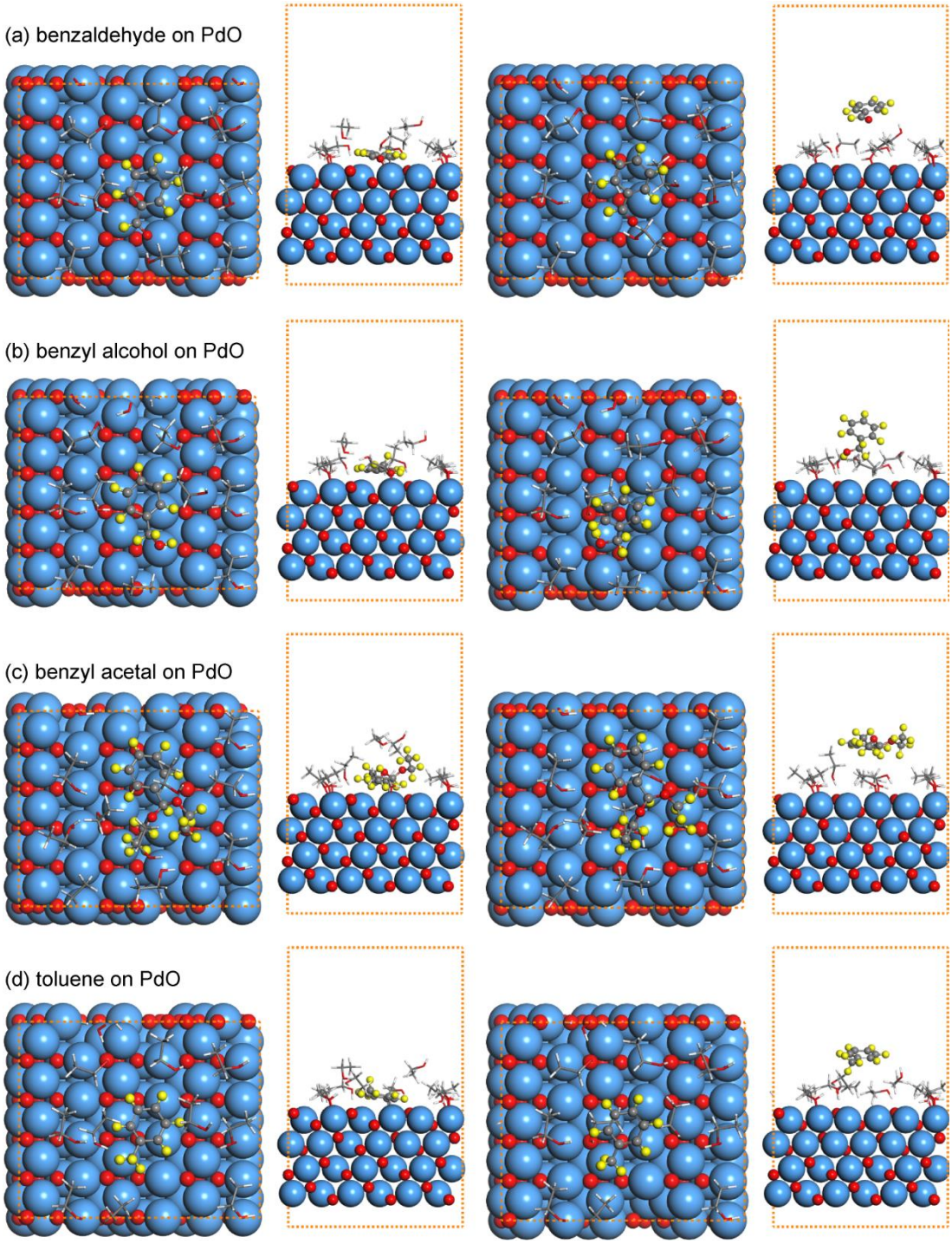

Supporting Figure S2. Optimized adsorption configurations of reactants, intermediates, and products with ten ethanol molecules on PdO surface by DFT calculations.

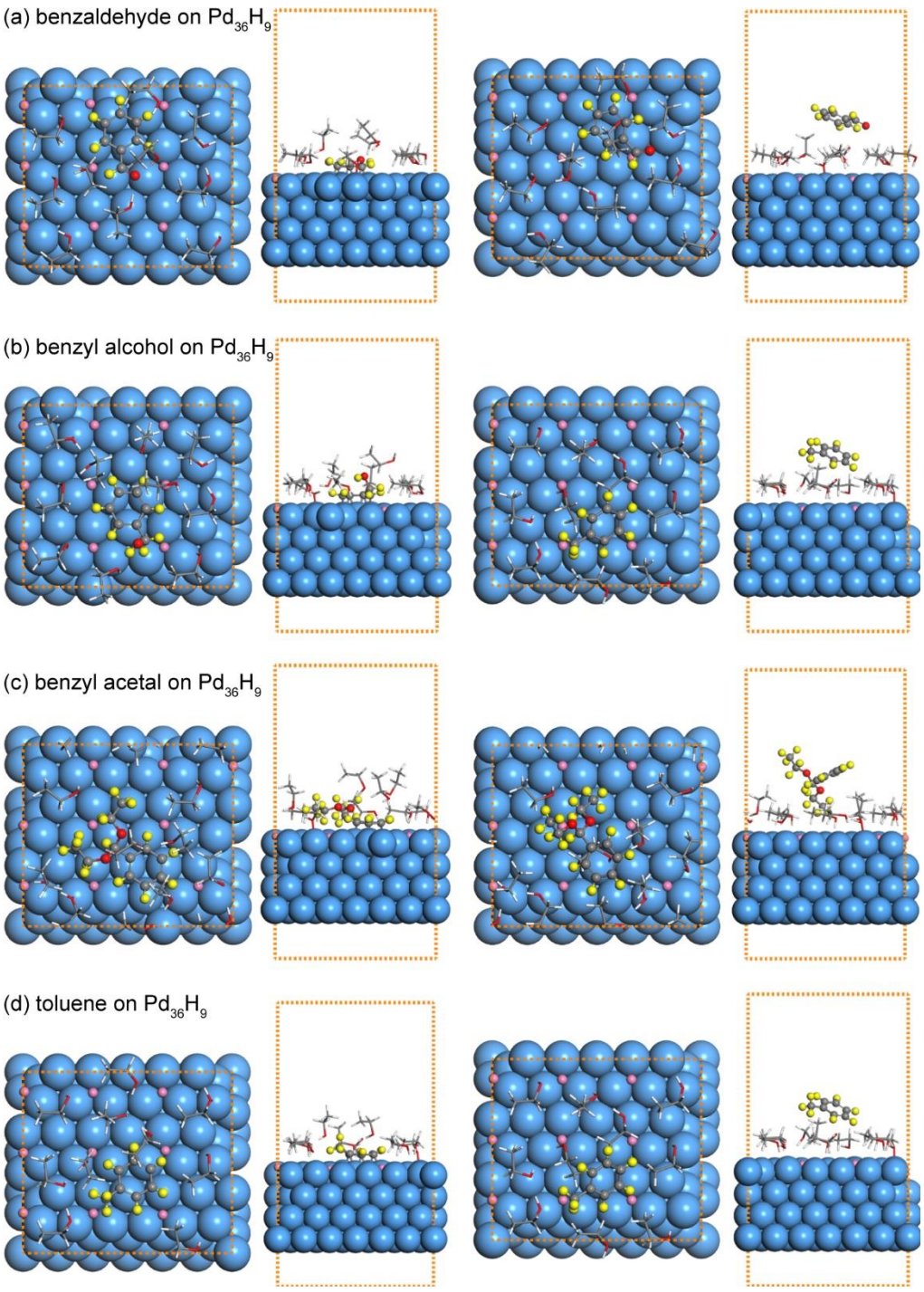

Supporting Figure S3. Optimized adsorption configurations of reactants, intermediates, and products with ten ethanol molecules on $Pd_{36}H_9$ surface by DFT calculations.

XPS analysis shows that only C, N, O, and Pd are detected from the survey spectra of Pd(II)/CN and PdH_X/CN (Fig. S4a). The C1s and N1s spectra of both samples are similar to that of pristine g-C_3N_4 (Fig. S4b and S4c).

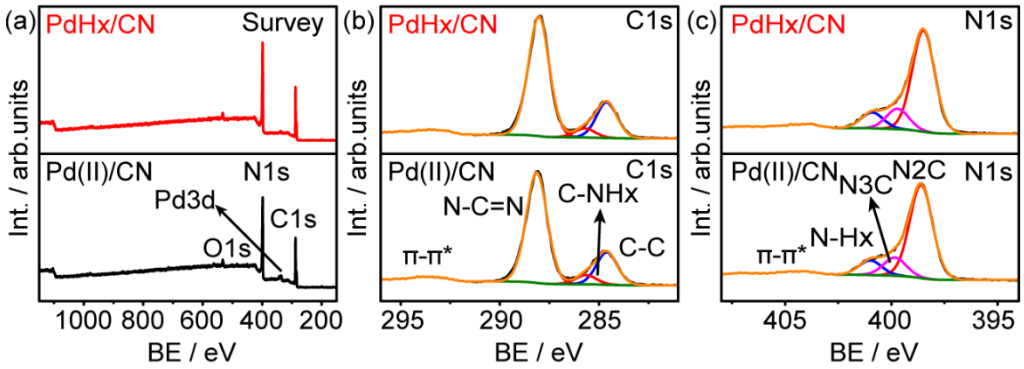

Supporting Figure S4. XPS analysis of the photocatalyst. (a)-(c) XPS survey, C1s and N1s spectra of the Pd(II)/CN and PdH_X/CN, respectively.

CV analysis shows that only the PdH_X/CN presents characteristic redox peaks in comparison with Pd(II)/CN and pristine g-C_3N_4 (Fig. S5).

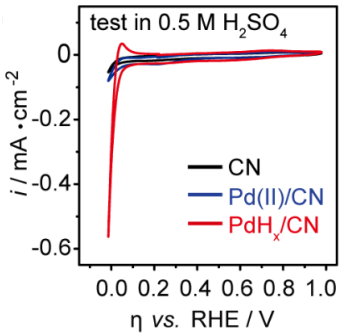

Supporting Figure S5. CV of the pristine CN, Pd(II)/CN and PdH_X/CN in 0.5 M H_2SO_4**.**

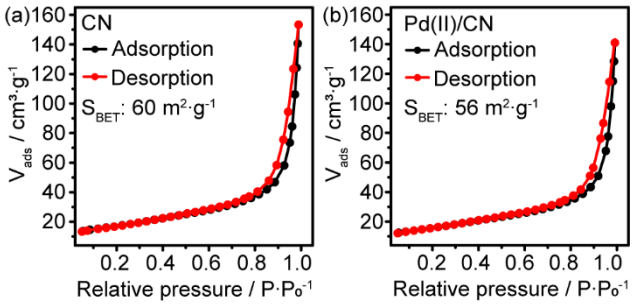

Supporting Figure S6. N_2 isotherms of the pristine CN and Pd(II)/CN**.**

XRD patterns show that the diffraction peaks at 12.9° and 27.4° can be assigned to the (100) and (002) lattice planes of g-C_3N_4, respectively (Fig. S7a). The diffraction peaks at 40.1°, 46.5°, and 68.0° are the (111), (200) and (220) lattice planes of Pd, respectively. A high resolution scan of the Pd(111) of both samples is shown in Fig. S7b.

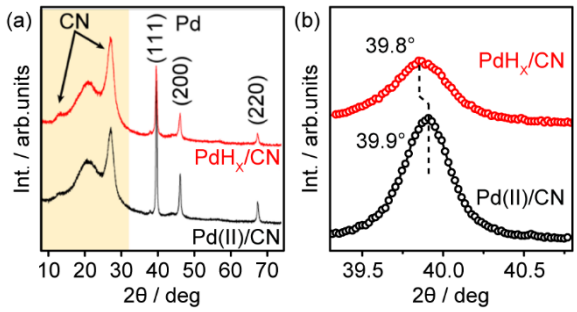

Supporting Figure S7. (a) and (b) XRD patterns of Pd(II)/CN and PdH_X/CN.

EDS mapping of the Pd(II)/CN is shown in Figure S8.

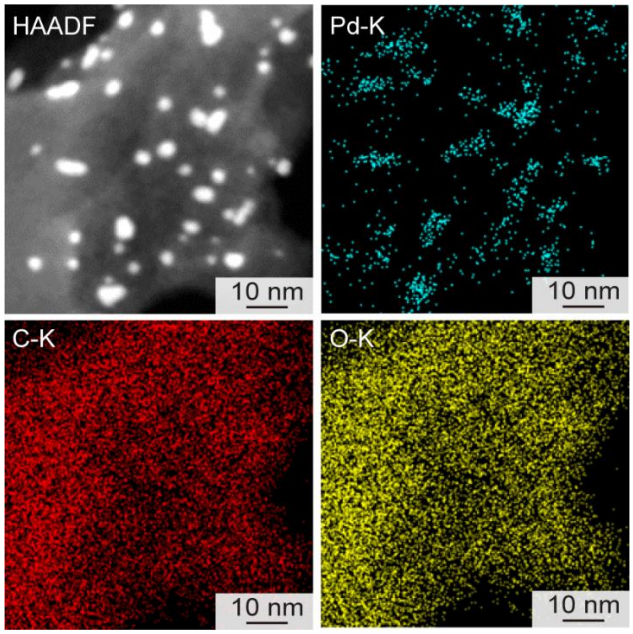

Supporting Figure S8. EDS mapping analysis of the PdH_X/CN photocatalyst.

The representative low resolution TEM images of Pd (II)/CN and PdH_X/CN are shown in Figure S9.

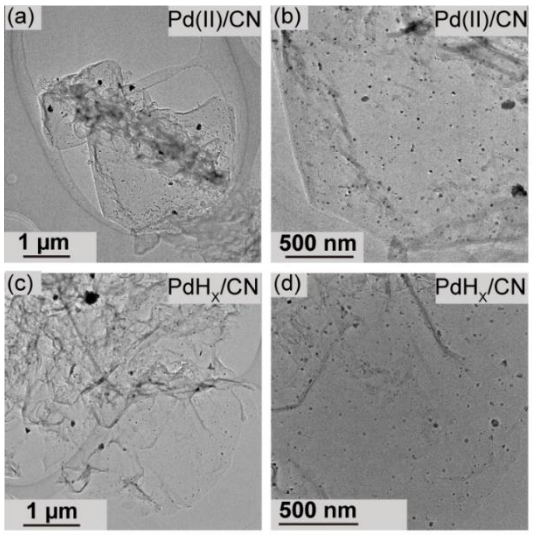

Supporting Figure S9. Low resolution TEM images of the Pd(II)/CN and PdH_X/CN.

Temperature programmed desorption (TPD) of benzaldehyde, benzaldehyde diethyl acetal, and benzyl alcohol on Pd(II)/CN are shown in Figure S10(a). TPD of benzaldehyde on pristine gCN is shown in Figure S10(b).

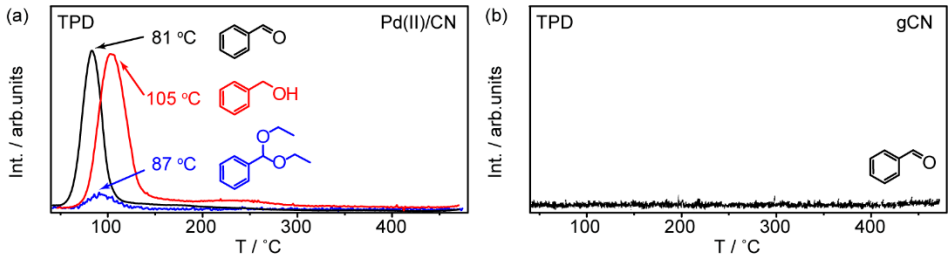

Supporting Figure S10. (a) TPD of benzaldehyde, benzyl acetal, and benzyl alcohol on Pd(II)/CN. (b) TPD of benzaldehyde on pristine gCN.

The effects of metal loading, concentration of catalyst, and irradiation wavelength for photocatalytic hydrogenation of aromatic ketones using Pd(II)/CN photocatalyst are shown in Figure S11. Pd(II)/CN photocatalysts with loadings of 1 and 3 wt% Pd can fully convert benzaldehyde into toluene within an irradiation time of 1 h (410 nm, Fig. S11a). A full conversion of benzaldehyde to toluene is achieved within 1 h of irradiation using 6 and 10 mg of Pd(II)/CN (3 wt%); however, an extended irradiation time of 2.5 h is required for 1g□L^{-1} of Pd(II)/CN (410 nm, Fig. S11b). Benzaldehyde can be converted to toluene under 365 and 410 nm irradiation within 1 h (Fig. S11c), but benzaldehyde diethyl acetal is the major product under 450 nm irradiation even for prolonged reaction time (5 h). Since the bandgap of gCN is ~2.7-2.8 eV, the near-edge excitation generated electrons may exhibit a fast recombination kinetics or tend to be trapped at the defect states, thus resulting in a poor catalytic performance.

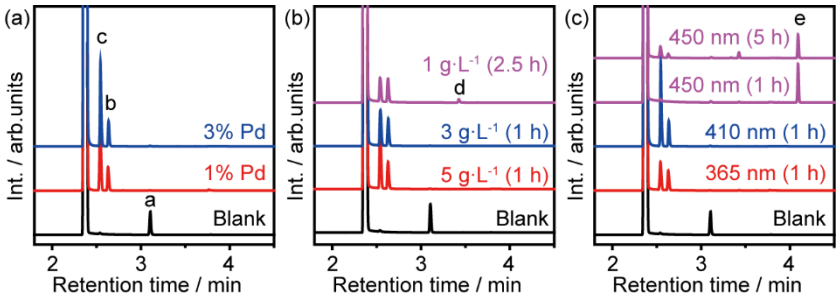

Supporting Figure S11. Photocatalytic conversion of benzaldehyde using Pd(II)/CN. (a)-(c) The effects of Pd loading, irradiation wavelength, and concentration of photocatalyst. Reaction conditions: 10 mM benzaldehyde in 2 mL ethanol solution under Ar atmosphere at RT. The labelled peaks are a: benzaldehyde; b: toluene; c: acetaldehyde diethyl acetal; d: phenyl ethyl ether; e: benzaldehyde diethyl acetal.

Photocatalytic conversion of benzaldehyde using glycerol as the hydrogen donor is performed using an identical reaction condition by replacing ethanol with a 50 vol% glycerol-water solution. A complete conversion of benzaldehyde into toluene is achieved within an irradiation course of 2 h, as confirmed by GC analysis shown in Figure S12.

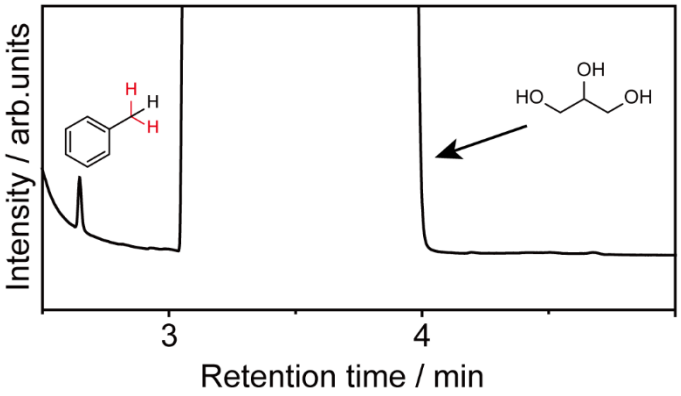

Supporting Figure S12. GC analysis of photocatalytic hydrogenation of benzaldehyde using glycerol as the hydrogen donor. Reaction conditions: 10 mg photocatalyst with 10 mM benzaldehyde in 2 mL glycerol-water solution (50 vol%) under 410 nm irradiation (14.8 mW·cm^{-2}) under Ar atmosphere at RT for 2 h.

Figure S13 shows the GC analysis of the liquid phase composition of each cycle during the reusability tests of photocatalytic hydrogenation of benzaldehyde over Pd (II)/CN. In the presence of HCl, the peak intensity of toluene remains unchanged within 10 cycles (Figure S13a). In the absence of HCl, the peak of toluene gradually decreased while the peak of benzyl alcohol increased (Figure S13b).

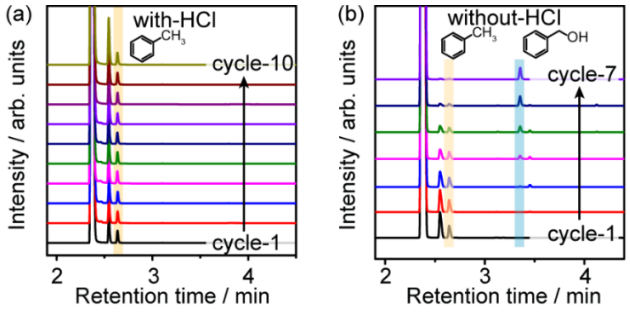

Supporting Figure S13. GC analysis of the liquid phase products during reusability tests of Pd(II)/CN for photocatalytic hydrogenation of benzaldehyde with (a) and without HCl (b).

Post-mortem analysis of the Pd(II)/CN in the presence of 0.5 vol% HCl in ethanol is shown in Figure S14.

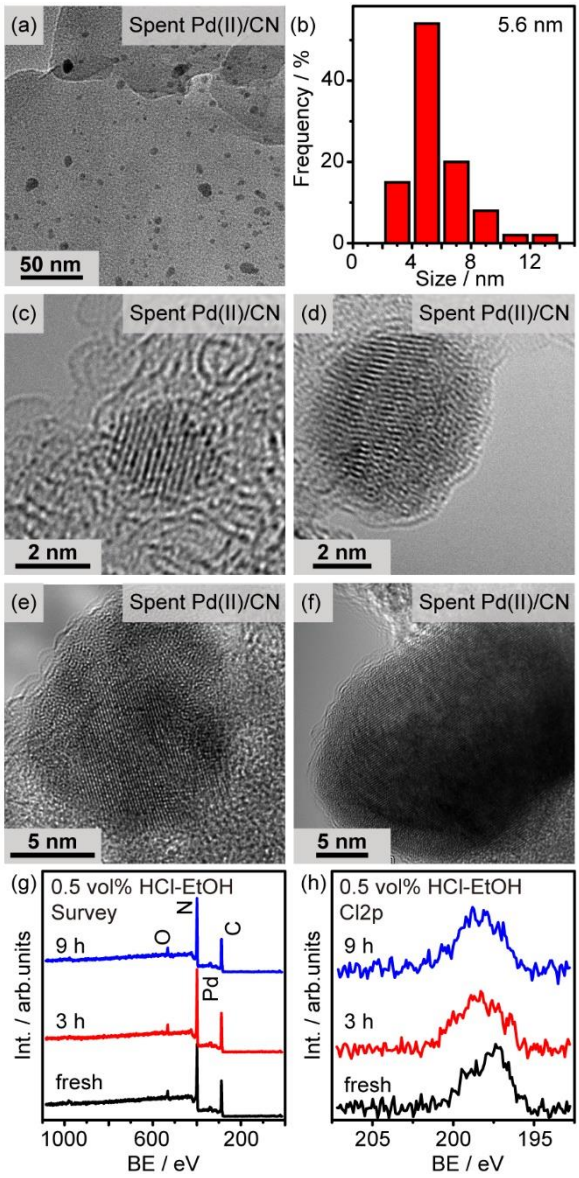

Supporting Figure S14. (a) and (b) TEM imaging and particle size distribution of the spent Pd(II)/CN. (c)-(f) HRTEM images of representative Pd NPs with different sizes. (g) and (h) XPS analysis of fresh and spent Pd(II)/CN with different irradiation time. The negligible amount of Cl is considered as Cl^- residuals. Photocatalytic reaction conditions: 10 mg Pd(II)/CN, 8 mM benzaldehyde in 2 mL 0.5 vol% HCl-ethanol solution at RT.

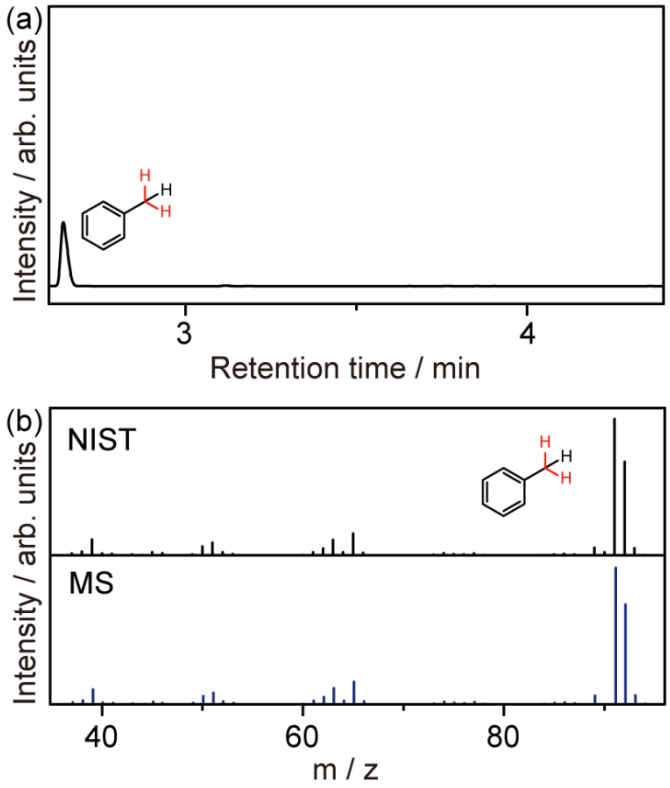

Supporting Figure S15. benzaldehyde as substrate. **(a)** GC data. **(b)** MS data.

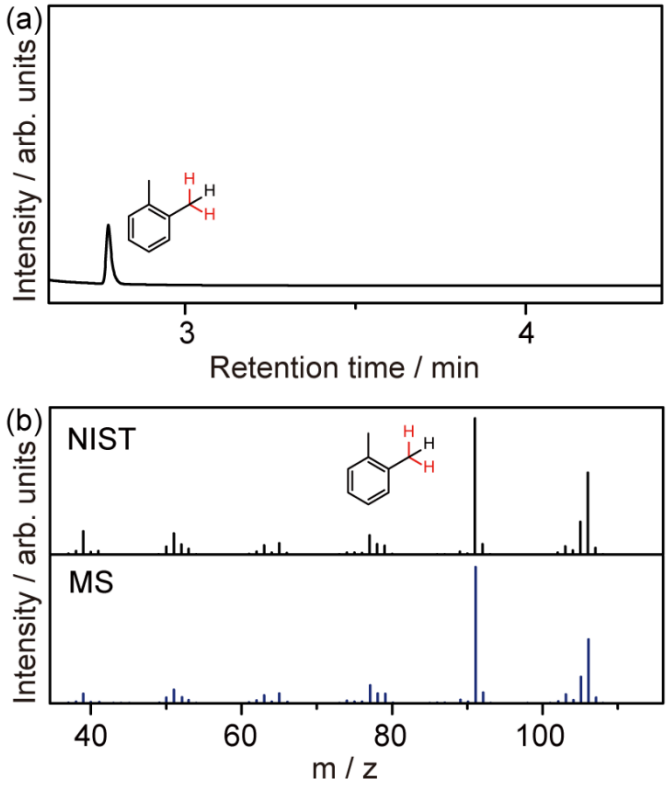

Supporting Figure S16. 2-methylbenzaldehyde as substrate. **(a)** GC data. **(b)** MS data.

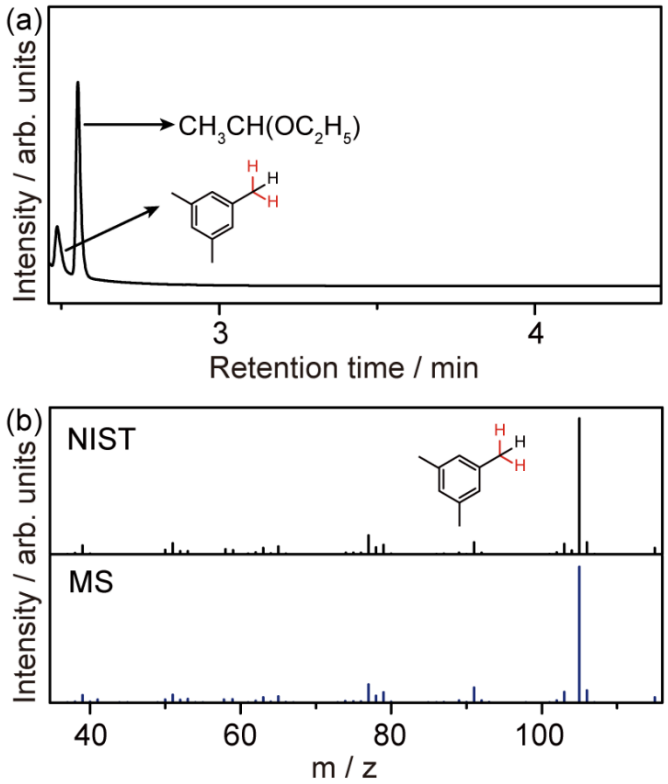

Supporting Figure S17. 3,5-dimethylbenzaldehyde as substrate. **(a)** GC data. **(b)** MS data.

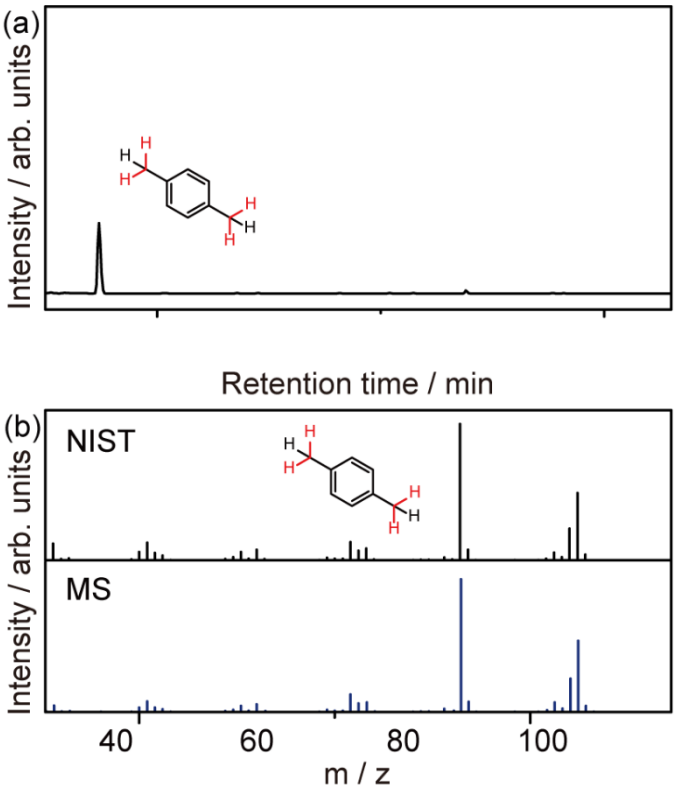

Supporting Figure S18. terephthalaldehyde as substrate. **(a)** GC data. **(b)** MS data.

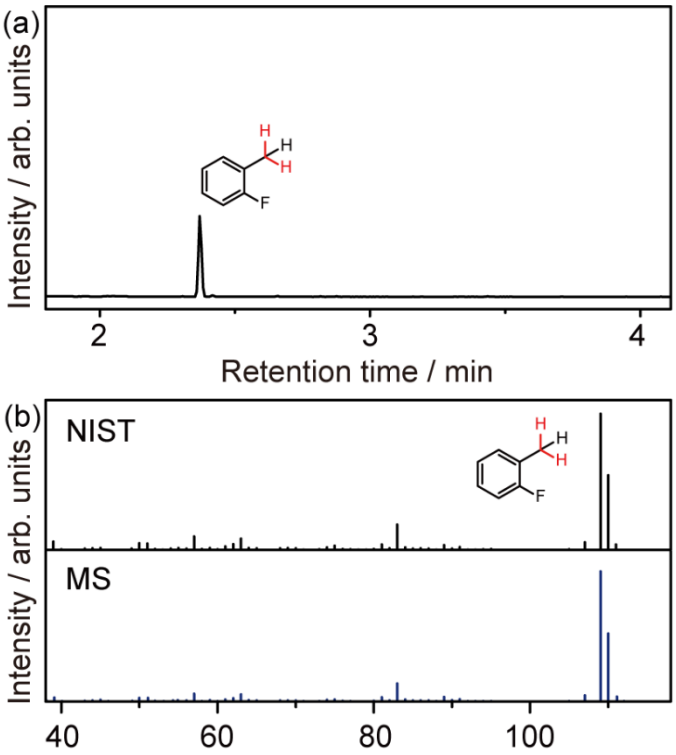

Supporting Figure S19. 2-fluorobenzaldehyde as substrate. **(a)** GC data. **(b)** MS data.

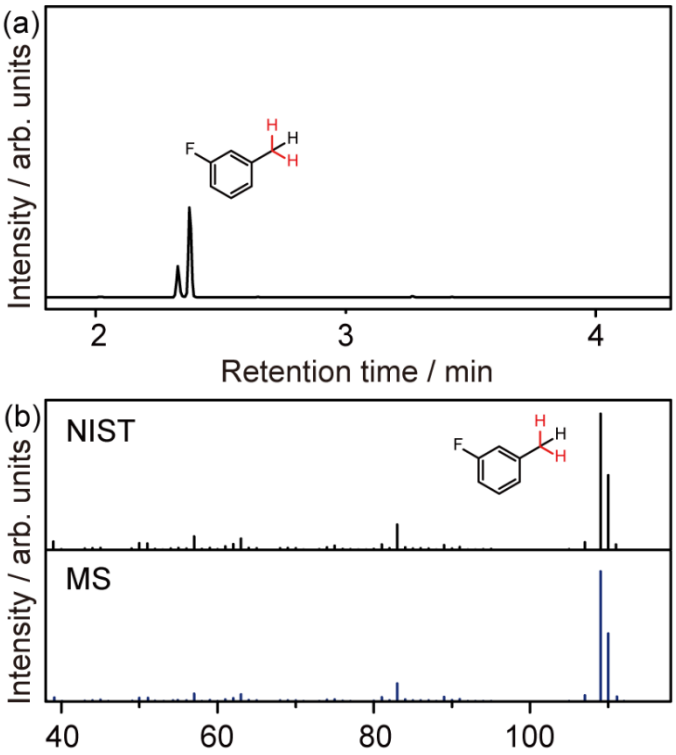

Supporting Figure S20. 3-fluorobenzaldehyde as substrate. **(a)** GC data. **(b)** MS data.

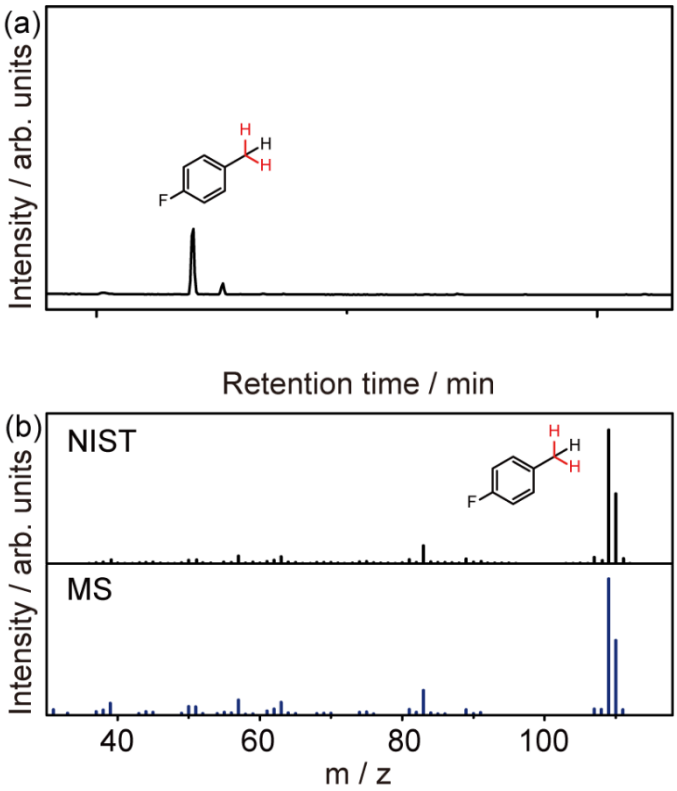

Supporting Figure S21. 4-fluorobenzaldehyde as substrate. **(a)** GC data. **(b)** MS data.

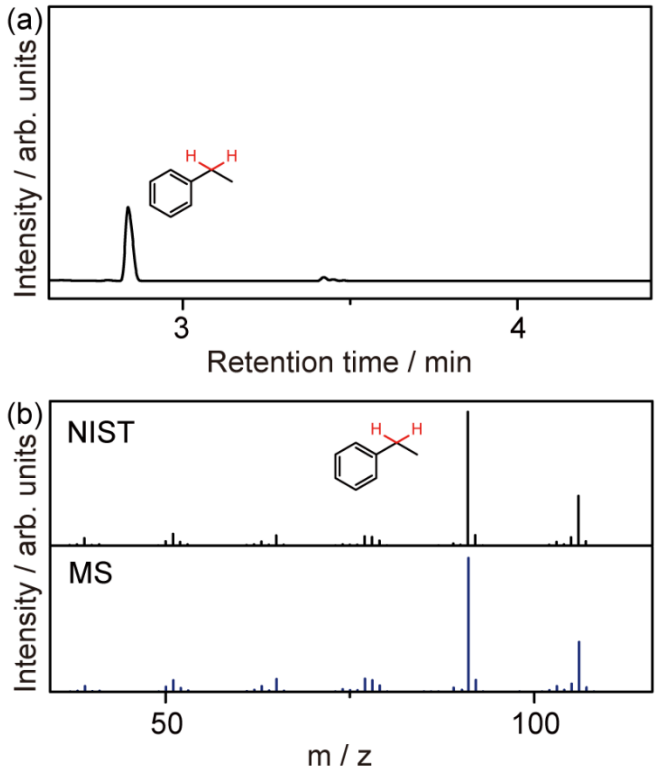

Supporting Figure S22. Acetophenone as substrate. **(a)** GC data. **(b)** MS data.

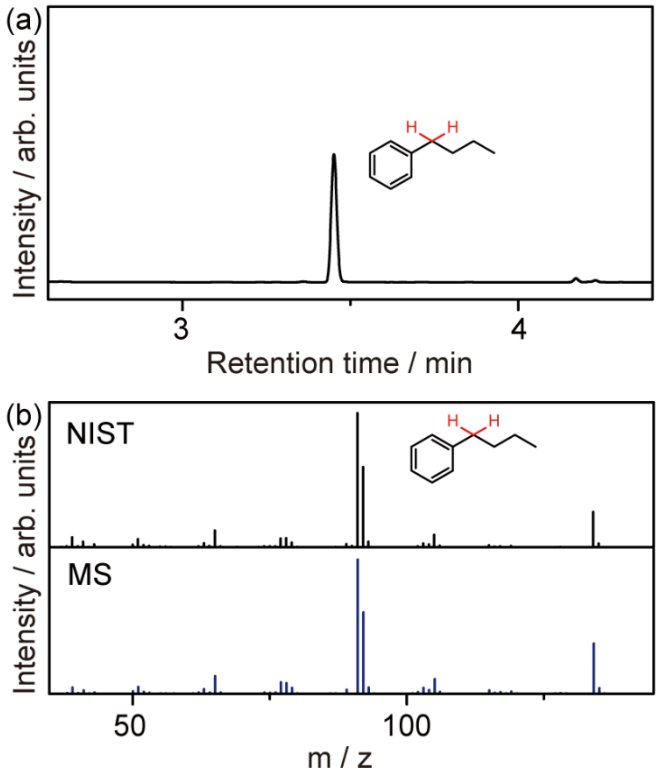

Supporting Figure S23. 1-phenylbutan-1-one as substrate. **(a)** GC data. **(b)** MS data.

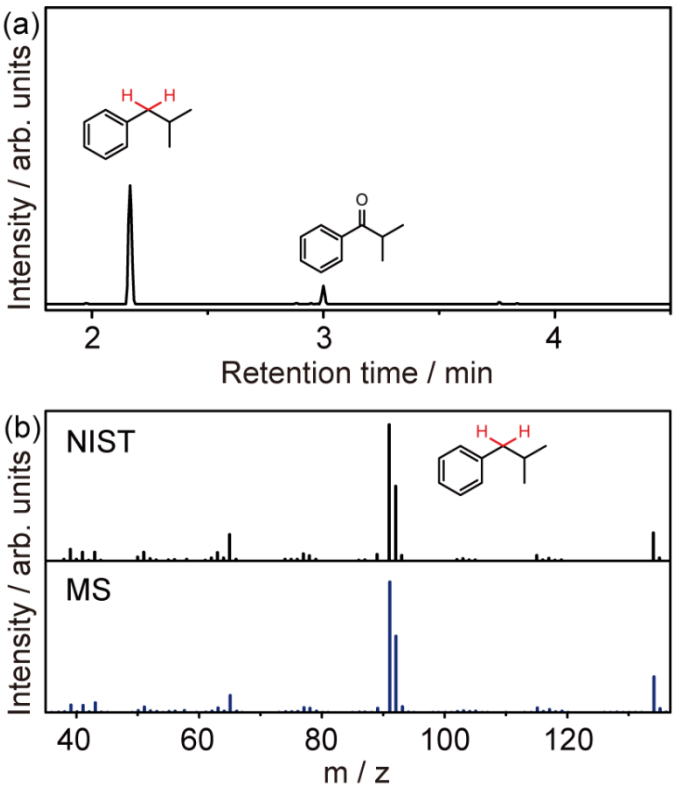

Supporting Figure S24. 2-methyl-1-phenylpropan-1-one as substrate. **(a)** GC data. **(b)** MS data.

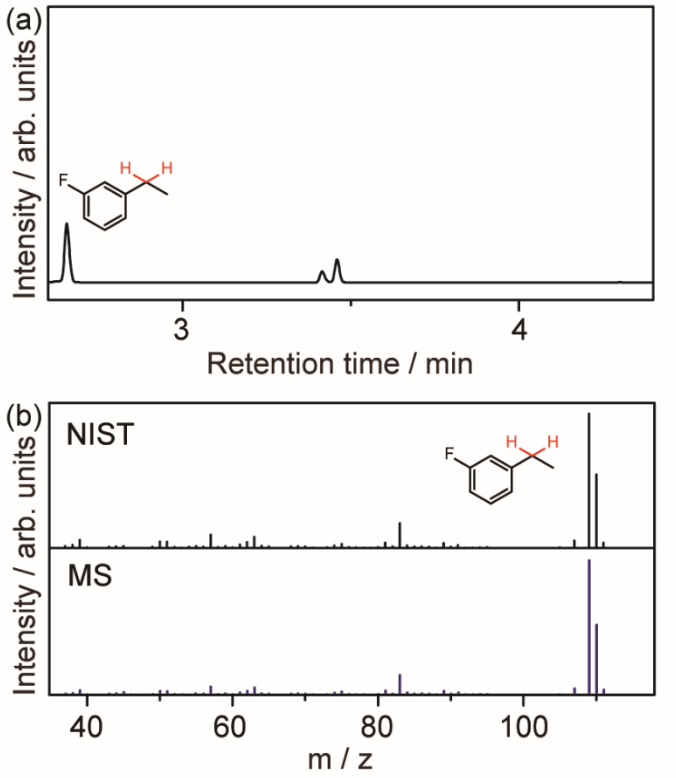

Supporting Figure S25. 1-(3-fluorophenyl)ethan-1-one as substrate. **(a)** GC data. **(b)** MS data.

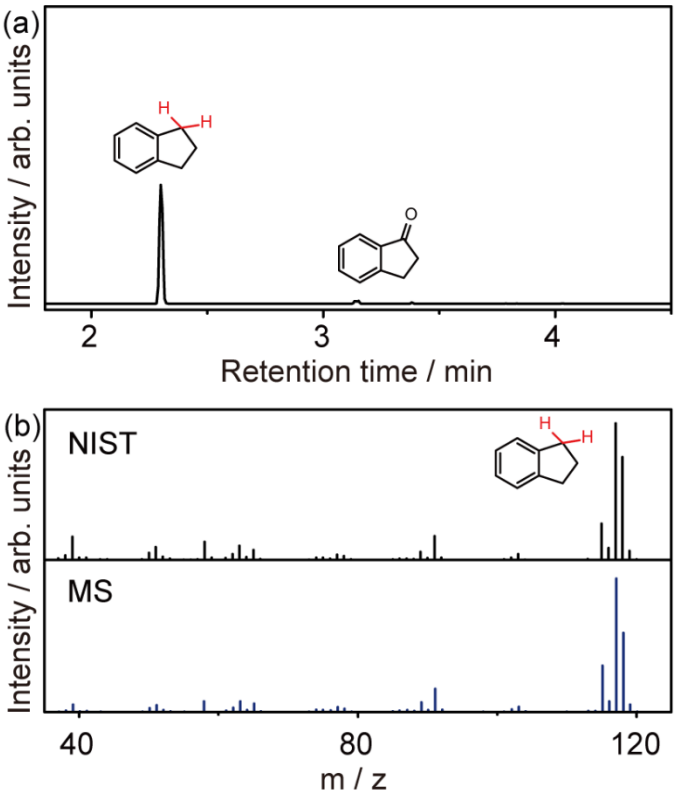

Supporting Figure S26 2,3-dihydro-1H-inden-1-one as substrate. **(a)** GC data. **(b)** MS data.

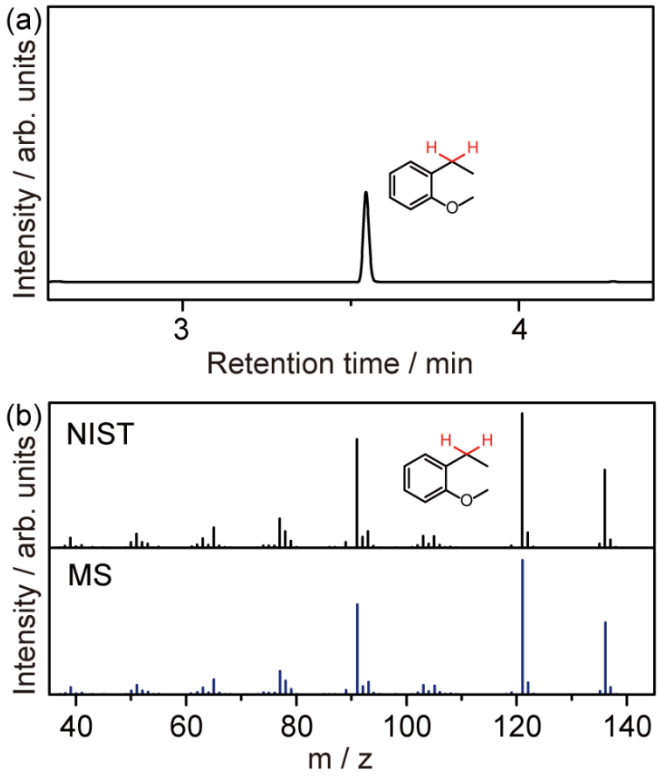

Supporting Figure S27. 1-(2-methoxyphenyl)ethan-1-one as substrate. **(a)** GC data. **(b)** MS data.

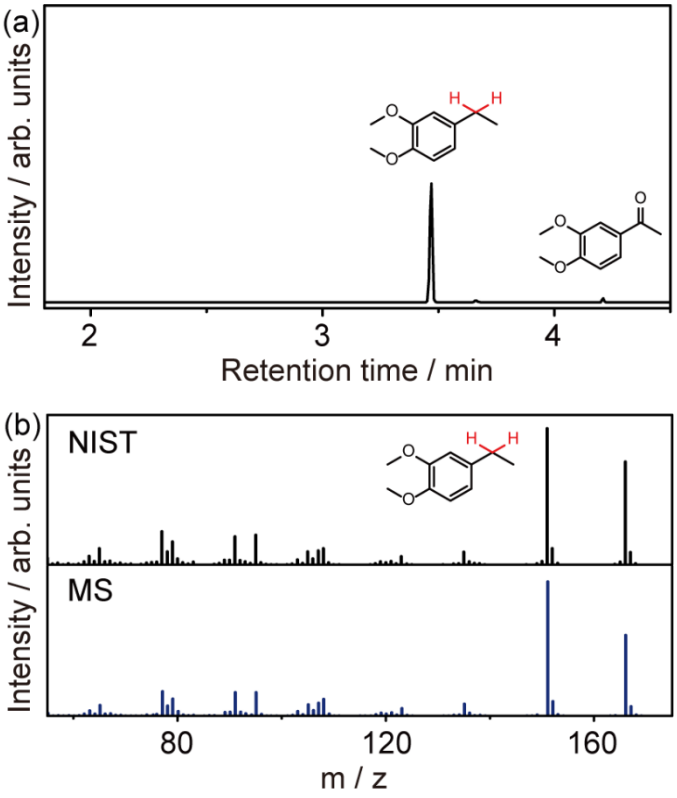

Supporting Figure S28. 1-(3,4-dimethoxyphenyl)ethan-1-one as substrate. **(a)** GC data. **(b)** MS data.

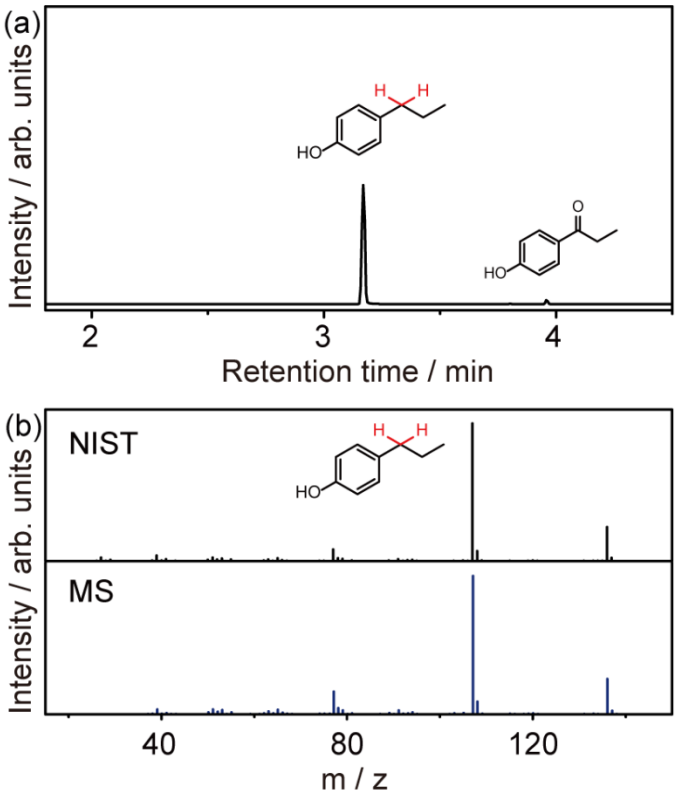

Supporting Figure S29. 1-(4-hydroxyphenyl)propan-1-one as substrate. **(a)** GC data. **(b)** MS data.

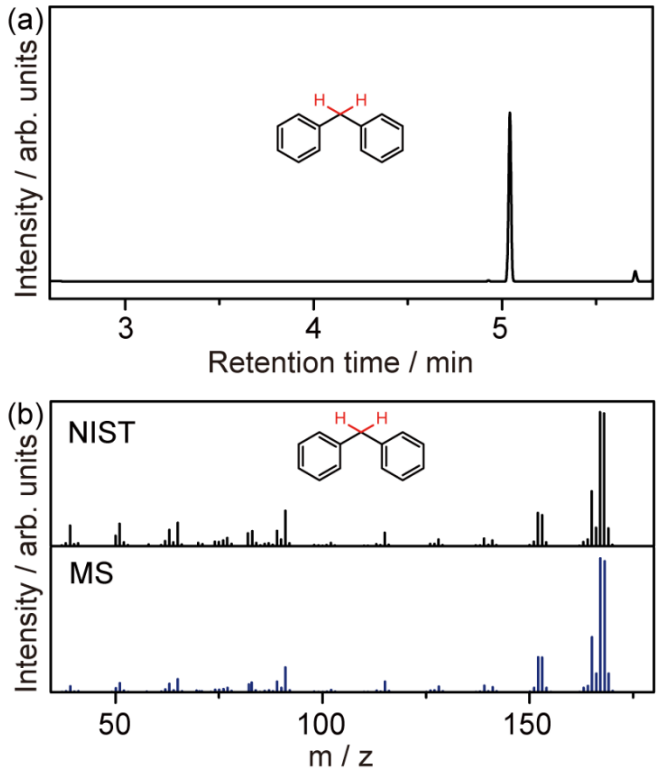

Supporting Figure S30. benzophenone as substrate. **(a)** GC data. **(b)** MS data.

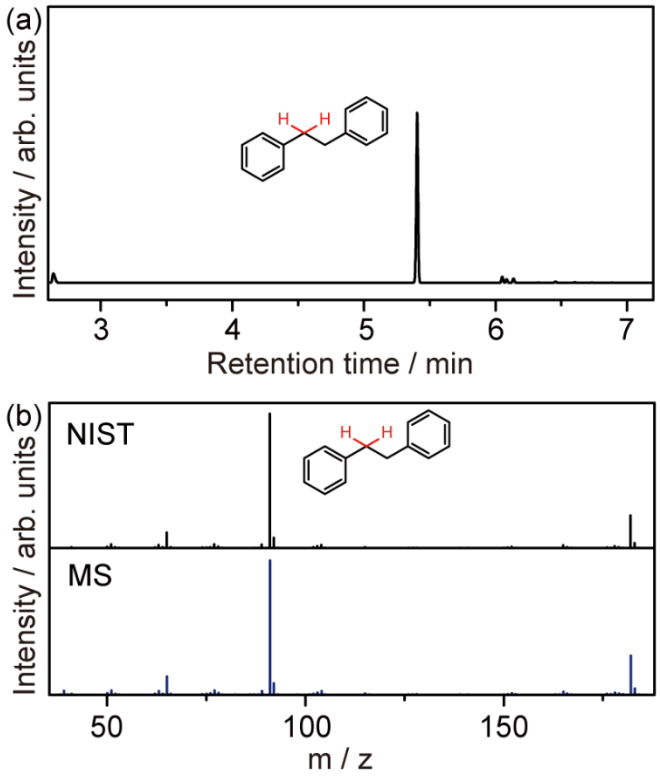

Supporting Figure S31. 1,2-diphenylethan-1-one as substrate. **(a)** GC data. **(b)** MS data.

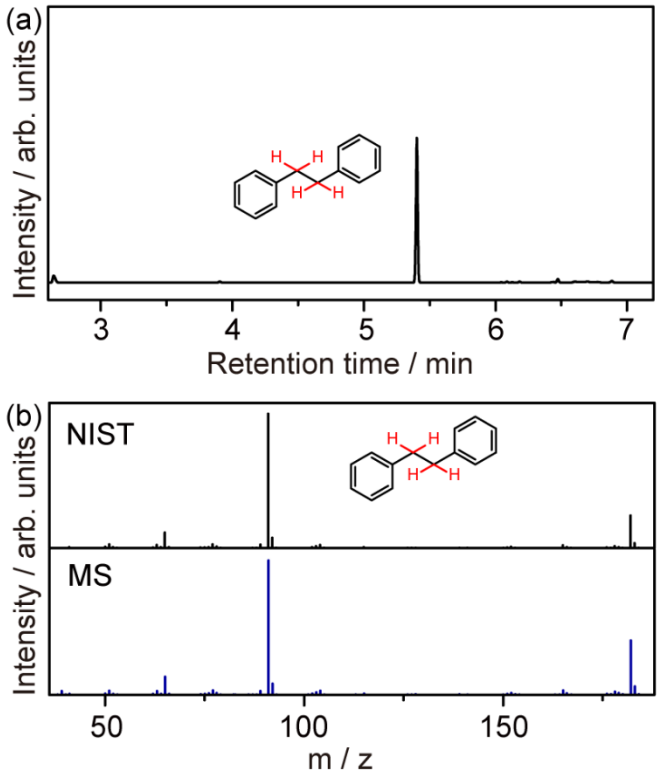

Supporting Figure S32. benzil as substrate. **(a)** GC data. **(b)** MS data.

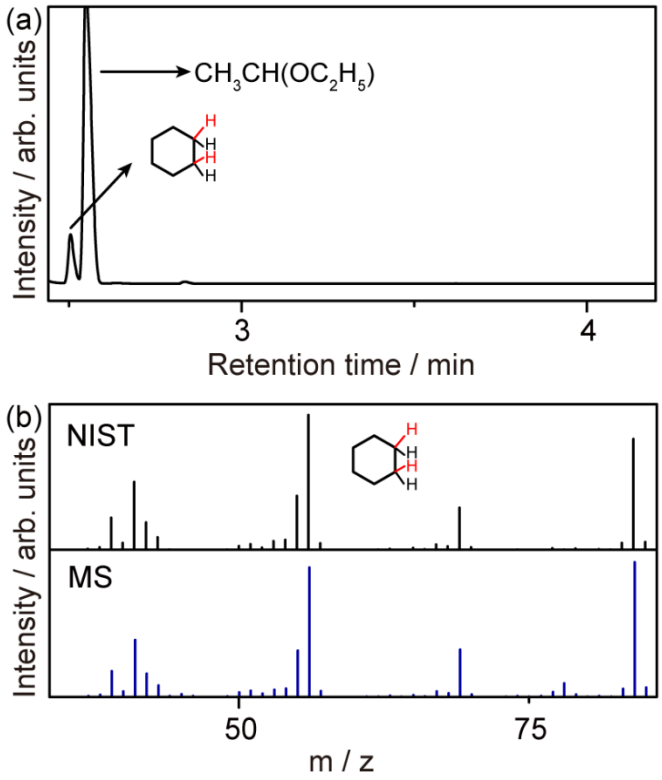

Supporting Figure S33. cyclohexene as substrate. **(a)** GC data. **(b)** MS data.

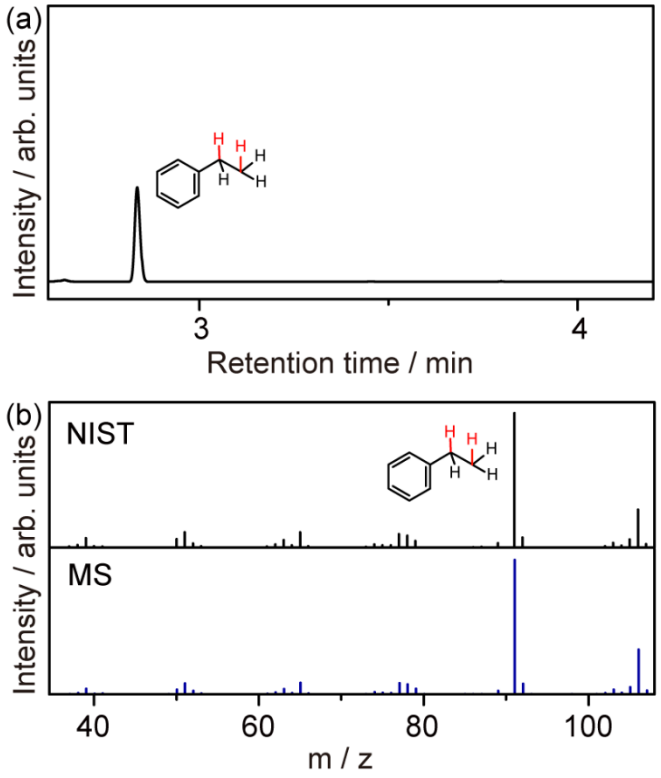

Supporting Figure S34. styrene as substrate. **(a)** GC data. **(b)** MS data.

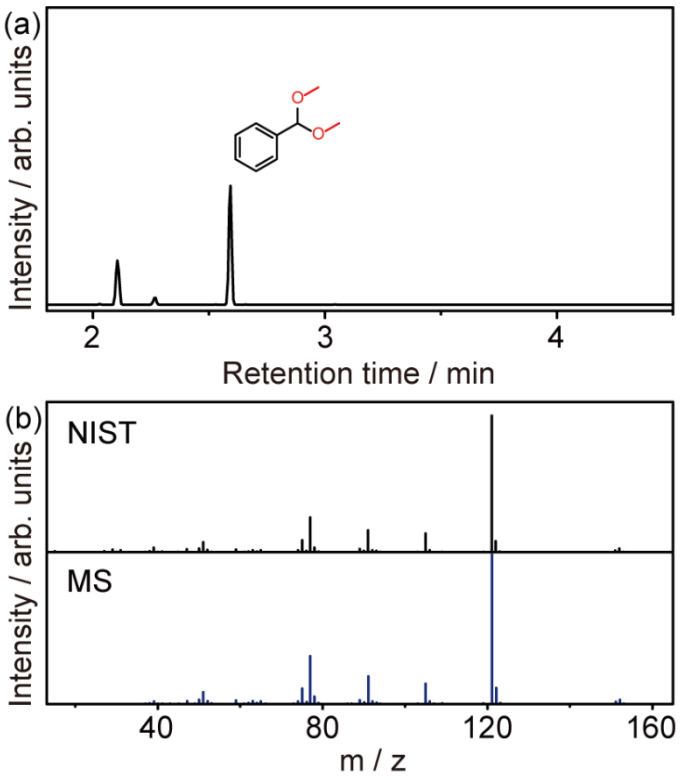

Supporting Figure S35. Methanol as substrate. **(a)** GC data. **(b)** MS data.

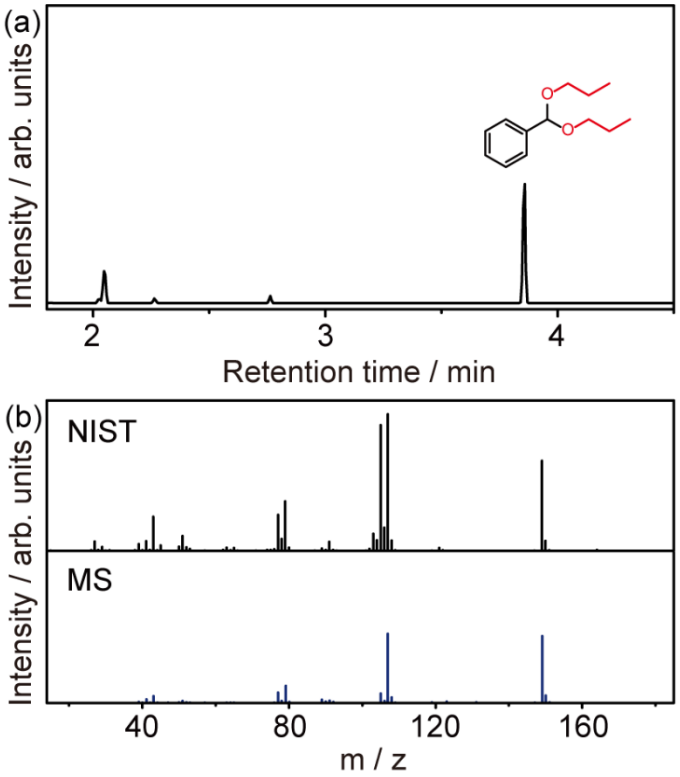

Supporting Figure S36. 1-Propanol as substrate. **(a)** GC data. **(b)** MS data.

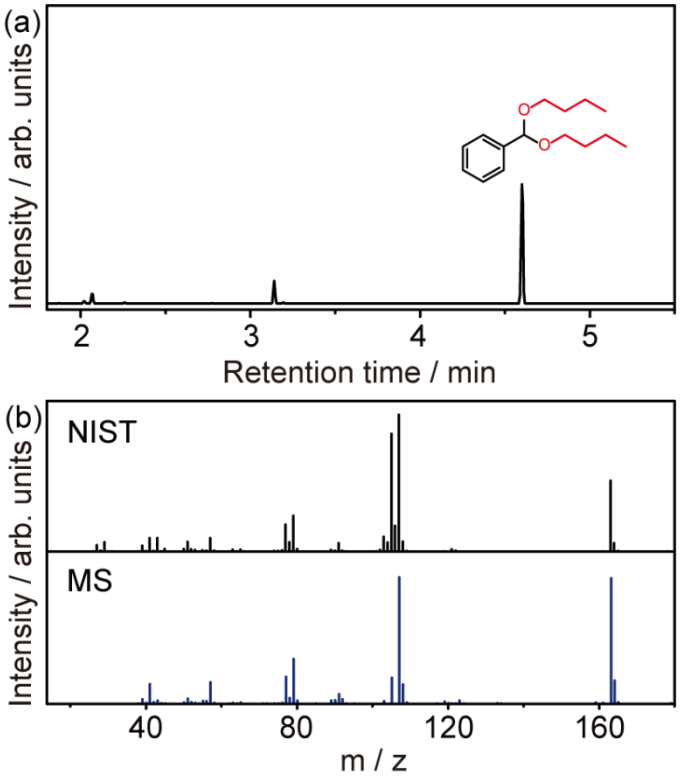

Supporting Figure S37. 1-Butanol as substrate. **(a)** GC data. **(b)** MS data.

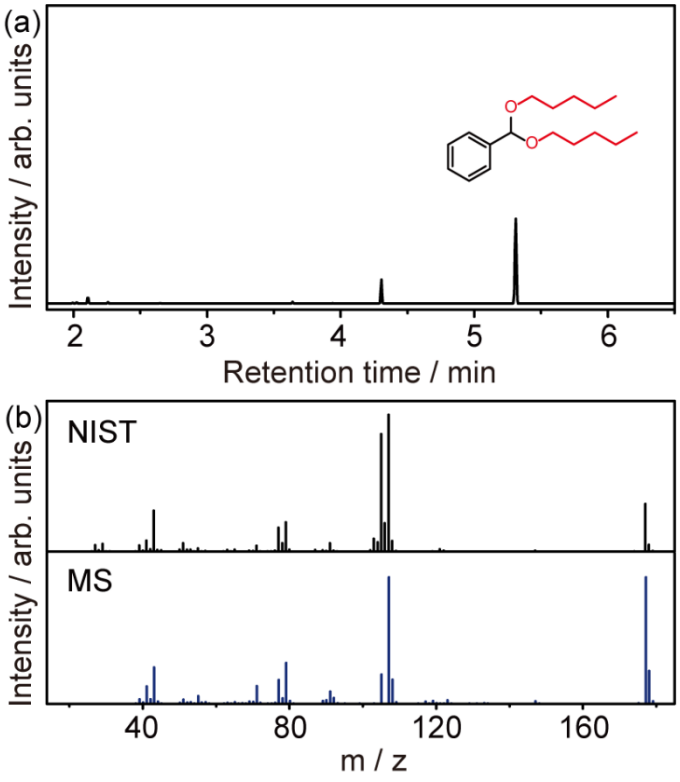

Supporting Figure S38. 1-Indanone as substrate. **(a)** GC data. **(b)** MS data.

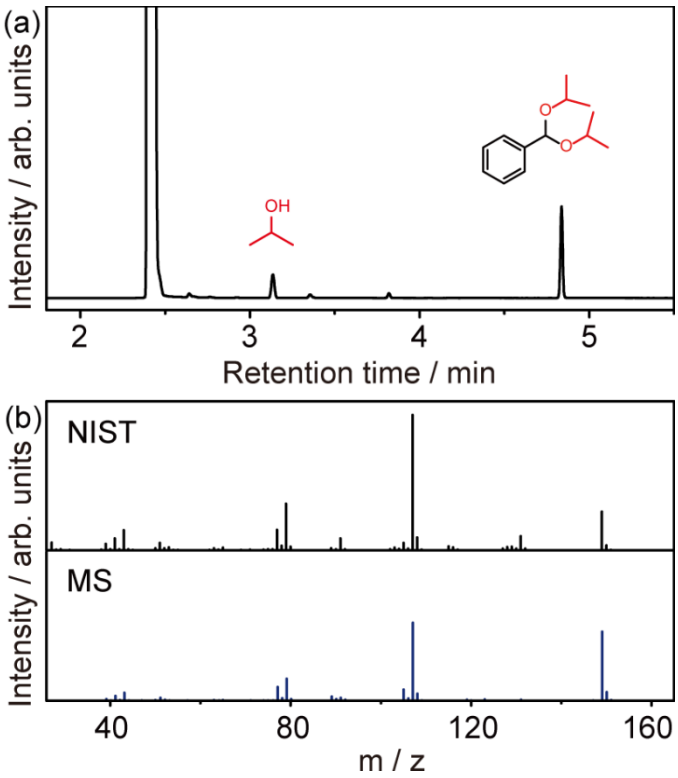

Supporting Figure S39. Isopropanol as substrate. **(a)** GC data. **(b)** MS data.

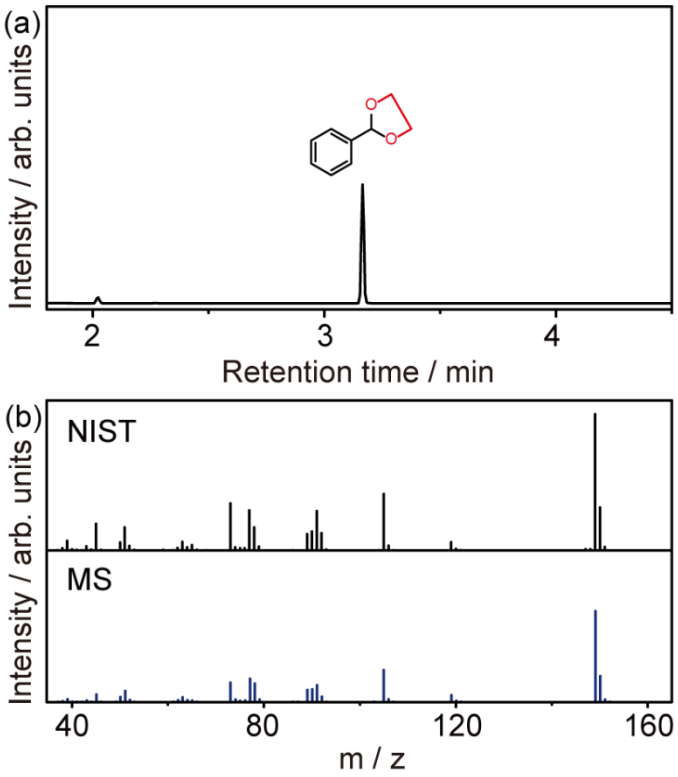

Supporting Figure S40. Ethylene glycol as substrate. **(a)** GC data. **(b)** MS data.

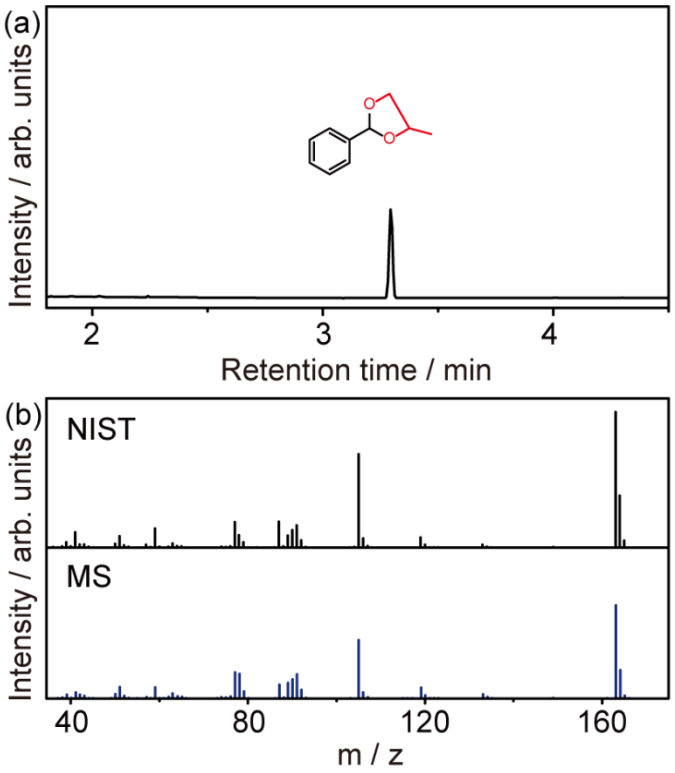

Supporting Figure S41. 1,2-Propanediol as substrate. **(a)** GC data. **(b)** MS data.

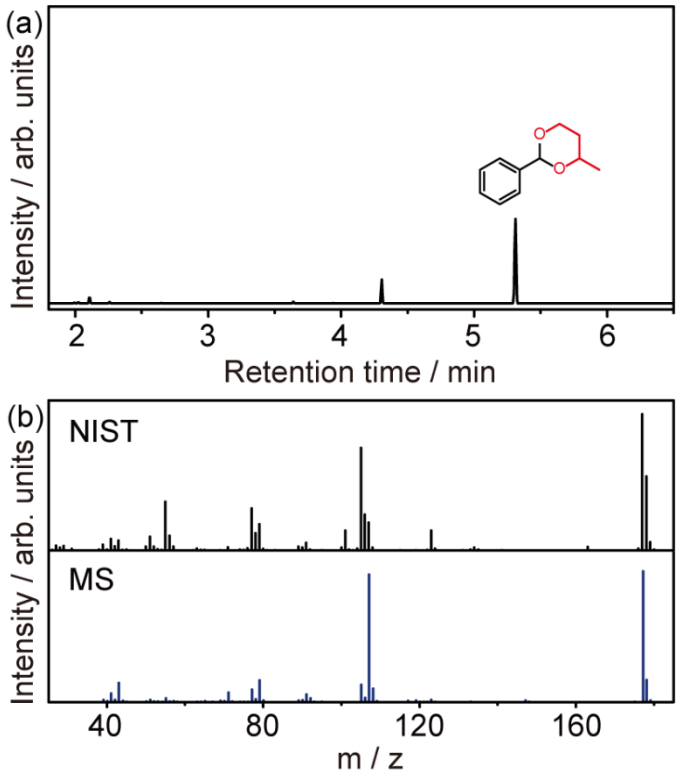

Supporting Figure S42. 1,3-Butanediol as substrate. **(a)** GC data. **(b)** MS data.

The raw data of *in-situ* mass spectra recorded during photocatalytic hydrogenation with and without benzaldehyde using both Pd(II)/CN and PdH_x/CN are shown in Fig. S43. H_2 (m/z =2), H_2O (m/z =18), N_2 (m/z = 28), CO_2 (m/z =44), and O_2 (m/z = 32) were recorded.

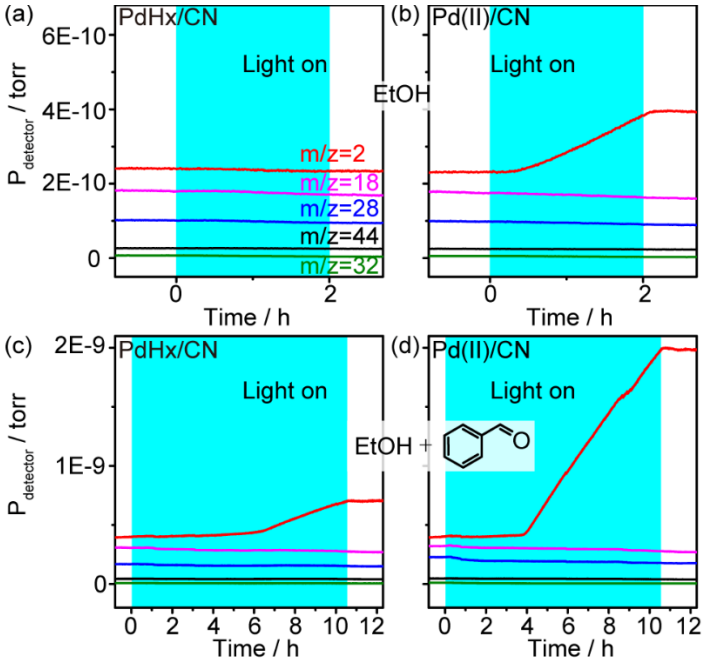

Supporting Figure S43. Time-resolved mass spectrometry recorded under irradiation using Pd(II)/CN and PdH_X/CN in pure ethanol (a and b), and with the presence of benzaldehyde (c and d).

4. Supporting Tables

Table S1 shows the calculated adsorption energies of reactant, intermediates, and product on Pd, $Pd_{36}H_9$ and PdO surfaces.

Table S1 Calculated adsorption energies of different reactants on various Pd surfaces.

Molecules	E_{ads} on Pd (eV)	E_{ads} on $Pd_{36}H_9$ (eV)	E_{ads} on PdO (eV)
C_2H_5OH	-0.90	-0.74	-1.27
Ph-CHO	-0.86	-0.55	-0.06
Ph-CH_2OH	-0.59	+0.15	-0.14
Ph-$CH(OCH_2CH_3)_2$	-0.86	-1.33	-0.09
Ph-CH_3	-1.19	-0.87	-0.53

Pd loading was determined using ICP-AES. The loading of Pd on PdH_X/CN and Pd(II)/CN are 3.3% and 3.4%, respectively, as shown in Table S2.

Table S2 ICP-AES analysis of Pd loading of PdH_X/CN and Pd(II)/CN

Samples	Pd / wt%
PdH_X/CN	3.3
Pd(II)/CN	3.4

As listed in Table S3, Pd loaded on either graphitic carbon nitride or TiO_2 can convert benzaldehyde into benzyl acetal with a high selectivity under heat, though the conversion efficiency is dependent on the support.

Table S3 Thermal catalytic conversion of benzaldehyde to benzaldehyde diethyl acetal.

Samples	Conversion / %	Selectivity / %
Pd(II)/CN	89	99
Pd/TiO_2	43	99

Reaction conditions: 10 mM reactant, 10 mg catalyst in 2 mL alcohol under 60 °C for 50 min in an inert atmosphere.

Supporting References

1 Kresse, G. & Furthmuller, J. Efficient Iterative Schemes for Ab Initio Total-Energy Calculations Using A Plane-Wave Basis Set. *Phys. Rev. B* **54**, 11169-11186 (1996).

2 Kresse, G. & Furthmuller, J. Efficiency of Ab-Initio Total Energy Calculations for Metals and Semiconductors Using A Plane-Wave Basis Set. *Comput. Mater. Sci.* **6**, 15-50 (1996).

3 Blochl, P. E. Projector Augmented-Wave Method. *Phys. Rev. B* **50**, 17953-17979 (1994).

4 Kresse, G. & Joubert, D. From Ultrasoft Pseudopotentials to The Projector Augmented-Wave Method. *Phys. Rev. B* **59**, 1758-1775 (1999).

5 Perdew, J. P., Burke, K. & Ernzerhof, M. Generalized Gradient Approximation Made Simple. *Phys. Rev. Lett.* **77**, 3865-3868 (1996).

6 Perdew, J. P. *et al.* Atoms, Molecules, Solids, And Surfaces - Applications of The Generalized Gradient Approximation for Exchange And Correlation. *Phys. Rev. B* **46**, 6671-6687 (1992).

7 Grimme, S., Antony, J., Ehrlich, S. & Krieg, H. A Consistent And Accurate Ab Initio Parametrization of Density Functional Dispersion Correction (DFT-D) for The 94 Elements H-Pu. *J. Chem. Phys.* **132**, 154104 (2010).

8 Wang, X. *et al.* Supramolecular Precursor Strategy for The Synthesis of Holey Graphitic Carbon Nitride Nanotubes With Enhanced Photocatalytic Hydrogen Evolution Performance. *Nano Res.* **12**, 2385-2389 (2019).

9 Zhang, D. *et al.* Photocatalytic Abstraction of Hydrogen Atoms from Water Using Hydroxylated Graphitic Carbon Nitride for Hydrogenative Coupling Reactions. *Angew. Chem. Int. Ed.*, **61**, e202204256 (2022).

10 Su, R. *et al.* Designer Titania-Supported Au–Pd Nanoparticles for Efficient Photocatalytic Hydrogen Production. *ACS Nano* **8**, 3490-3497 (2014).

11 Li, Y. *et al.* Rationally Designed Metal Cocatalyst for Selective Photosynthesis of Bibenzyls via Dehalogenative C–C Homocoupling. *ACS Catal.* **11**, 4338-4348 (2021).